Ocean Engineering 313 (2024) 119521

Contents lists available at ScienceDirect

Ocean Engineering

journal homepage: www.elsevier.com/locate/oceaneng

Research paper

Buoys for marine weather data monitoring and LoRaWAN communication

Arnas Majumder, Michele Losito, Santhosh Paramasivam, Amit Kumar *, Gianluca Gatto

Department of Electrical and Electronic Engineering, University of Cagliari, 09123, Cagliari, Italy

ARTICLE INFO

Keywords:
Smart moored weather buoys
Low power wireless sensor network
LoRaWAN gateway
Sustainable energy harvesting systems
Water quality
IoT based environment monitoring and data analytics

ABSTRACT

Climate change not only affects the environment directly but also challenges the existence of human civilization. Changes observed in the marine environment indicate the planet's health. Continuous ocean observations (ambient conditions, water quality, aquatic life, and disaster management) are crucial for checking and balancing climate change. This research aims to design three prototype smart moored buoys suitable for environmental monitoring. During the project, biconical buoys with a diameter of 30 cm and a height of 80 cm were fabricated. The buoys were fitted with temperature, salinity, and pH sensors to monitor and gather meteorological data. The collected data is transmitted to the cloud environment through a wireless communication device which is installed in all buoys through a LoRaWAN gateway, where it is stored and retrieved for analysis. The energy requirement of these buoys for driving the sensor network and data transmission are taken care by harvesting the solar energy through photovoltaic panels and the secondary energy storage device housed in the buoy. These buoys are installed along the coast in the municipality of Villasimius, Sardinia, Italy. These buoys have been placed within the marine protected area of Capo Carbonara, Sardinia, Italy, at a suitable distance from the communication gateway.

1. Introduction

Observation of ocean is essential to monitor its health and to track global climate change. Due to the rise in global temperature, the glaciers and ice sheets are melting rapidly, and together with the thermal expansion of seawater, sea levels are also rising significantly (Lindsy). Since 1880, the global mean sea level did rise approximately by 21–24 cm. Whereas in some specific cases, this rise was noticed about 15–20 cm since the satellite recording started (Lindsy).

Marine pollution due to eutrophication, acidification, toxins, and the presence of plastics are notably responsible for damaging the ocean and rivers' aquatic environment and also causing harm to aquatic life worldwide (Verma et al., 2020). Whereas the decline in coastal water quality further poses substantial risks to coastal ecosystems and communities (D et al., 2022). On the other hand, Saltier oceans, together with greenhouse gases (CO_2 and CH_4), can lead to warmer climates (Olson et al., 2022). Therefore, ocean water salinity must be studied and monitored continuously, as highlighted in (Klemas, 2011), whereas measuring Sea Surface Salinity (SSS) is crucial in understanding oceanic biological and physical processes, such as global water balance, oceanic currents, and evaporation rates. In 1990, the World Ocean Circulation Experiment (WOCE) was established with goals (1) To develop models useful for predicting climate change and to collect the data necessary to test them and (2) To determine the representativeness of the specific WOCE data sets for the long-term behavior of the ocean, and to find methods for determining long-term changes in the ocean circulation (World Ocean Circulation Experiment). To achieve peace and prosperity for people and the planet, 17 Sustainable Development Goals (SDGs) were laid by the United Nations (UN) in 2015. The motto of the goal number 14 (GOAL 14) among all SDGs is "Conserve and sustainably use the oceans, seas, and marine resources for sustainable development."

Weather buoys primarily function as mini weather stations and are also known as marine environmental buoys or Coastal Weather Buoys (CWB) (Maritime Engineering Technology et al., 2019). While they are mostly equipped to collect meteorological (air temperature, wind direction, wind speed, maximum wind gusts, atmospheric pressure, relative humidity) or oceanographic (mean wave direction, wave height and period, maximum wave height and wave period, sea temperature, water salinity) data or both simultaneously (Maritime Engineering Technology et al., 2019) (Kuznetsov) (Winchester, 1974). Weather buoys are classified into two categories based on their mounting techniques. The first type, the drafting buoy, has a spherical-shaped body with a diameter

* Corresponding author.
E-mail addresses: arnas.majumder@unica.it (A. Majumder), michele.losito@unica.it (M. Losito), santhosh.paramasivam@unica.it (S. Paramasivam), amit.kumar@unica.it (A. Kumar), gatto@unica.it (G. Gatto).

https://doi.org/10.1016/j.oceaneng.2024.119521
Received 8 July 2024; Received in revised form 5 October 2024; Accepted 13 October 2024
Available online 18 October 2024

ranging from 0.3 m to 0.4 m and is known to be built with ABS plastic (Maritime Engineering Technology et al., 2019). This type of buoy moves freely with ocean currents and has been in use since 1972 (Oceanic Engineering Society and Marine Technology Society, 2013). On the other hand, the second type, the moored buoys, have a discus-shaped body with diameters ranging from 0.3 m to 0.4 m and are particularly anchored to the ocean floor and built of aluminum or ionomer foam (Maritime Engineering Technology et al., 2019).

The buoys also can be sub-classified based on their specific applications to collect information on the marine environmental conditions like: (1) Ocean Weather data buoys (Kington and Selinger, 2006): These buoys are designed to collect weather data, such as wind speed and direction, air temperature, humidity, air pressure, and precipitation. They are useful for monitoring weather conditions offshore and in coastal areas; (2) Surface drifting Oceanographic data buoys (Elipot et al., 2022): These buoys are placed on the ocean surface, and data such as surface water temperature, salinity, sea currents, wave heights, and meteorological parameters are collected. They provide information on surface oceanographic conditions and are useful for studying interactions between the ocean and the atmosphere; (3) Deep oceanographic data buoys (The proceedings of the twenty-first, 2011): These buoys monitor oceanographic conditions at greater depths. They can be equipped with sensors to measure water temperature, salinity, and pressure at different depths. They also study ocean stratification, deep currents, and other key oceanographic parameters; (4) Tsunami data buoys (Balaji et al., 2006): These buoys are specifically designed to detect and monitor seismic activity and the presence of tsunamis in the ocean. They can include pressure sensors and accelerometers to detect sea-level changes and provide early warnings of a potential tsunami; (5) Biological data buoys (Stohs and Harmon, 2022): some buoys collect data on the ocean's biological conditions. They can include sensors to detect the presence of algae, chlorophyll, phytoplankton, dissolved oxygen levels, and other biological characteristics that help monitor the health of marine ecosystems. According to the National Data Buoy Center (NDBC), a total of 1324 weather stations (buoys) (US Dept of Commerce) are deployed around the globe to measure meteorological and oceanographic data (see Fig. 1).

Oceanic metrological predictions and experimental forecasting started in the 1950s (Fathi et al., 2022), and significant progress has been made in the field of research and development of weather buoys. Notably, the literature reports a huge number of experimental and research works and the implementation of innovative weather-monitoring systems (buoys) in oceans (McLeod and Ringwood, 2022), (Lin and Yang, 2020) and rivers (Soreide et al., 2001). Some interesting notable research works are available on types, applications, and development of weather buoys are presented in (Maritime Engineering Technology et al., 2019), (Fathi et al., 2022), (McLeod and Ringwood, 2022), (Lin and Yang, 2020), (Soreide et al., 2001), (Malek Azari et al., 2020), (Xu et al., 2022), (Bojic et al., 2021), (NOAA et al., 2023). Small, low-cost, and lightweight wave buoys were fabricated to operate near the coast Hope, G. et al. (2024) (Klemas, 2011). In another study, Kodaira, T. et al. (2023) (Kodaira et al., 2024) have designed wave buoy for the study of wave-ice interactions. Similar low-cost multisensor monitoring buoy system proposed in (Albaladejo et al., 2012) to measure both atmospheric and marine pressures and temperatures. Zhong, Y.Z. et al. (2022) (Zhong et al., 2022) have made miniature wave buoys to measure the wind speed and wind direction. Whereas the low-cost Global Navigation Satellite System (GNSS) buoy used by Knight, P.J. et al. (2021) (Knight et al., 2021) to collect the sea level and wave data within the intertidal zone. The wind, wave, and marine current energy resources, etc., are monitored using a Sensor Buoy System, as reported by García, E. et al. (2018) (García et al., 2018). While in (Shukla et al., 2023) Shukla, A. et al. (2023) have proposed a self-energy harvesting buoy platform for the river Ganga's health monitoring and hazard prediction. In Balakrishnan Nair T.M. et al. (2024) (Balakrishnan Nair et al., 2024), authors have proposed an integrated buoy-satellite system for water quality observation and promoting a blue economy. Sun, Y. et al. (2024) (Sun et al., 2024) have proposed a disposable portable buoy that bridges the data transmission between underwater equipment (at a depth of 4000 m) and onshore laboratories. In (Jung et al., 2024) Jung, H. et al. (2024) presented a prototype self-powered ocean buoy incorporating a disk-type soft-contact mechanical frequency regulator TENG (DSMFR-TENG), a microcontroller, a temperature sensor, and an acoustic transmitter. Chen, S. et al. (2023) (Chen et al., 2023) have developed a PV-powered self--counterweight transverse-tethered semi-submersible prototype buoy; the buoy is equipped with a radiance radiometer (in water), irradiance radiometer (in water), altitude sensor, and depth sensor.

Interestingly in (Hurst et al., 2012), the authors installed a buoy with a weather station in Ruapehu Crater Lake; the measurements were conducted to confirm the estimations made on wind speed and solar radiation used in previous heat and mass balance calculations. Xie, X. et al. (2022) (Xie et al., 2022) used drafting air-sea interface buoy to collect the extreme air-sea turbulent fluxes during tropical cyclones in the South China Sea. Expendable micro SWIFT buoys have been developed by Thomson, J. et al. (2024) (Thomson et al., 2024) for the measurement of ocean surface waves. Notably, numerical investigations (Amaechi et al., 2022a),(Qin et al., 2019), (Amaechi et al., 2022b), (Ju

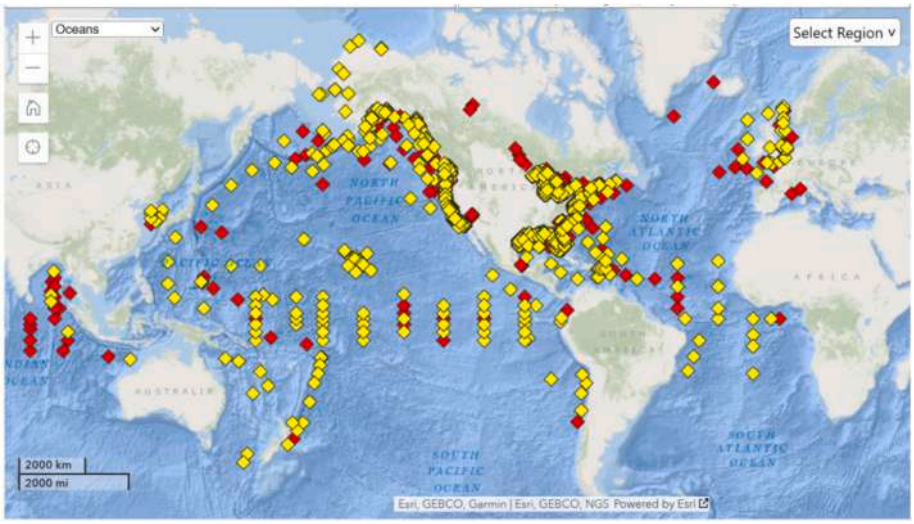

Fig. 1. *Different weather buoys deployed around different oceans,* US Dept of Commerce (US Dept of Commerce).

et al., 2023), (Amaechi et al., 2022c) are crucial for developing and implementing buoys and for analyzing buoy-gathered data. These studies primarily utilize mathematical models and simulations to forecast and assess buoy performance in diverse marine settings.

Effective communication for a buoy is paramount for ensuring safety, facilitating data collection, coordinating systems, environmental preservation, and enabling prompt emergency response. Consequently, it serves an indispensable and pivotal element within maritime operations and environmental monitoring. In order to carry out their functions efficiently, buoy systems are reliant upon a variety of communication technologies to transmit and receive information. The primary types of buoy communication technologies are as follows: (1) Radio communication (Song et al., 2016); (2) Satellite communication: telemetry systems (Martínez-Osuna et al., 2021), iridium satellite network (Kodaira et al., 2024) (Thomson et al., 2024) (Rabault et al., 2022), Global Positioning System (GPS) (Klemas, 2011); (3) Acoustic communication: Underwater Acoustic Modems (Otero et al., 2023); (4) Cellular Network communication (Przybysz et al., 2020); (5) Wireless Sensor Networks (WSNs) (Xu et al., 2014); (6) Optical Communication (Song et al., 2016): light-based systems, visible light (Darlis et al., 2018) or infrared (Kahn and Barry, 1997) (Chen et al., 2024); (7) Long Range (LoRa) Wireless Technology: Long Range Wide Area Network (LoRaWAN) (Nilo, 2020); (8) Internet of Things (IoT) modules and protocols (Kim et al., 2017) (P et al., 2023) (Santhosh et al., 2021).

This paper presents research and development, installation, and monitoring of a prototype weather buoy by the Department of Electrical and Electronic Engineering (DIEE), University of Cagliari (UniCA). Notably, this is for the first time, when a prototype buoy was installed near Sardinian Island (the marine protected area of Capo Carbonara) to collect the local meteorological data. The buoys featured in this paper are designed to be lightweight, energy-efficient, and self-sustaining, whereas they are built to transmit substantial data volumes with minimal maintenance. Its innovation/novelty lies in using LoRaWAN technology, which is known for its efficient data transmission and power conservation. Furthermore, its capability to operate in areas lacking GSM coverage enhances its versatility.

Subsequently, based on the experience gained from prototype buoy fabrication, the UniCA team is currently developing a smart weather cum docking station consisting of the moored buoy (mother) and a portable buoy (daughter). The mother buoy would work as a continuous working and communication station and host the daughter buoy. On the other hand, the daughter buoy would conduct long-distance missions, mainly to collect the water samples and analyze the presence of microplastics in the local seawater around Sardinia. It would also function as a moving weather station.

The paper is structured as follows: it starts with a brief introduction. Then, the project instrumentations are explained in section 2. The results and observations are highlighted in section 3. Section 4 discusses the future development of a combined fixed-moored buoy and portable mission buoy, while the final remarks are underlined in Section 5.

2. Instrumentation

A total of three weather buoys have been fabricated at the DIEE laboratory of the UniCA, Italy. While only two weather buoys were installed within the marine protected area of Capo Carbonara (Fig. 2), Sardinia, Italy. Figs. 3 and 4 show the Buoy 1 and Buoy 3 deployment locations. Fig. 5a shows the illustration of the installed sensors and instruments in the weather buoy, and Fig. 5b shows flowchart of methodology adopted in development and deployment of weather buoy. Table 1 presents various electronic components that have been installed inside the buoy to collect data i.e., (a) air temperature, (b) water temperature, (c) water pH, (d) buoy position (GPS), (e) battery status; (f) status of the Photovoltaic (PV) energy harvesting system; and (g) electrical measurements for the sole purpose of monitoring the consumption of prototypes.

The functional device has been installed in the buoy inside a protective casing (IP67). Additionally, a two-component protective gel has been applied to protect the electronic components from the local marine ambient and rough weather conditions.

Notably, the aforesaid device is an IoT (Internet of Things) object connected to a LoRa network, operating in the (European free) frequency range of 868 MHz, and it allows coverage in free air up to 10 km in radius. Whereas a LoRaWAN gateway has been installed along the coast in the municipality of Villasimius, while the buoys have been placed within the marine protected area at a suitable distance that allows communication with the gateway.

The network architecture considered for this project is a star type, where the star center corresponds to the LoRaWAN gateway while the endpoints are the LoRaWAN devices installed inside the buoys (see Fig. 6).

Both buoys (Fig. 7) are equipped with PV energy harvesting system and a battery storage system. Whereas the energy harvester has the task of recovering the energy needed to recharge the storage system, ensuring the battery's useful life enhancement. Notably, the buoys electronic system consists of: (1) ten miniaturized PV modules positioned on the outer surface of the buoy; (2) DC-DC conversion sections (one for each voltage level); (3) a microcontroller for managing the

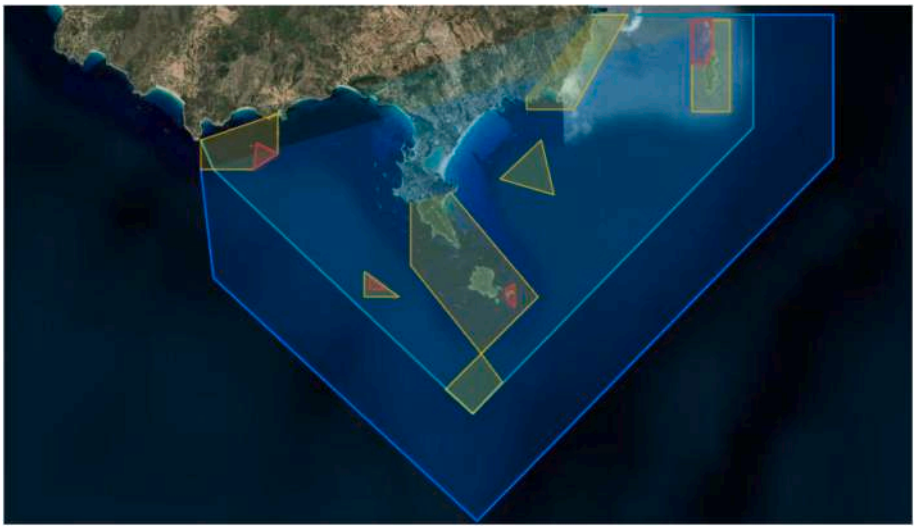

Fig. 2. The marine protected area of Capo Carbonara, Italy.

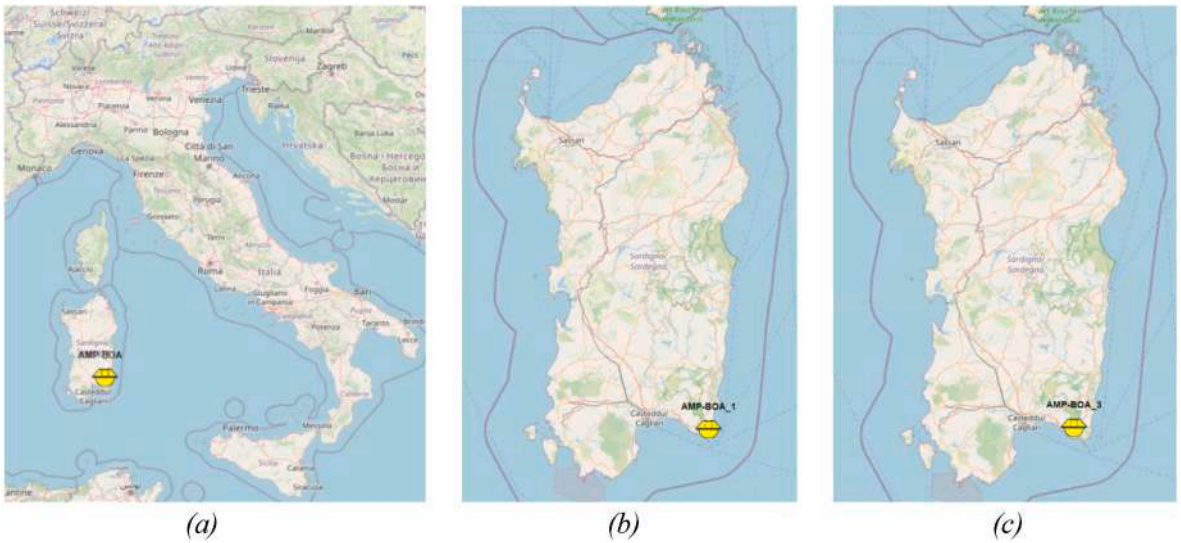

Fig. 3. (a) Buoy's location, (b) Buoy 1, and (c) Buoy 3.

Fig. 4. Zoomed view of the installations of the (a) Buoy 1 and (b) Buoy 3.

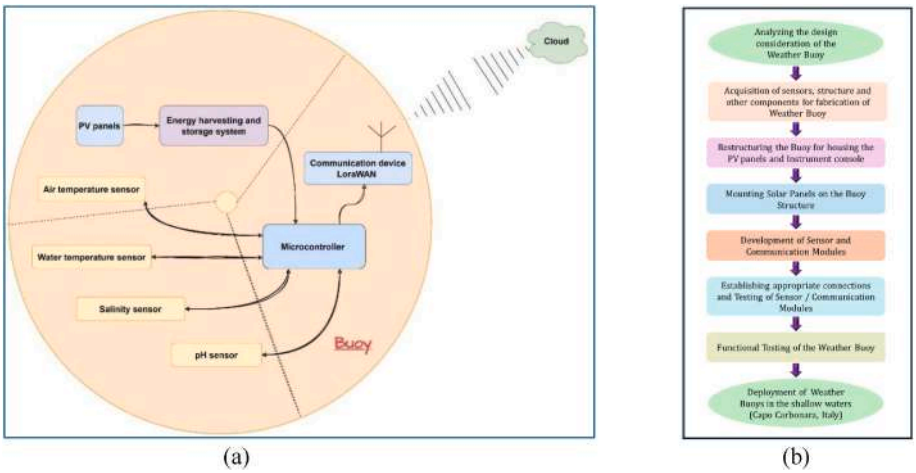

Fig. 5. (a) Illustration of the installed sensors and instruments in the weather buoy, and (b) Flowchart of Methodology adopted in development and deployment of weather buoy.

entire system; (4) a LoRaWAN modem, including the antenna; (5) an electronic device for measuring electrical parameters; (6) two temperature sensors for the air inside the buoy and one integrated into the pH measuring probe for measuring the water temperature; (7) a sensor for pH measurement; (8) a GPS device with its antenna, and (9) two electronic enclosures protected against the effects of continuous immersion at a depth of 1 m.

2.1. Construction of the smart buoy

The bi/conical buoy (as in Fig. 8a), was considered to construct three moored buoys weather-station to host the PV panels (Fig. 8b), various

Table 1
Instruments used for weather buoys.

Instruments	Type	Specification
PV panels	Poly	0.5W, 5V@100 mA
Battery	LiPo	7.4 V, 5200 mAh, 80 c
2 Air temperature sensor	DS18B20	10 °C to +85 °C (±0.5 °C); 3.5 – 5V DC
Water temperature sensor	ES-2 Electrical Conductivity &	3.3 V, 15 mA3; 0.995 mA (Sleep mode)
Water salinity sensor	Temperature Sensor	3.3 V; 15 mA3; 0.09 mA (Sleep mode)
Water pH	pH analog sensor with pH meter	3.3 V; 35 mA3; 0.4 mA (Sleep mode)
Energy harvester	BQ24650	
Bidirectional Current/ Power Monitoring Chip	INA219	
Microcontroller 1	Atmel ATmega328P	
Microcontroller 2	Arduino MKR WAN 1310	
Radio communication	LoRa	

sensors (Fig. 8c) and electronic devices (Fig. 8c & d).

The biconical buoys were cut horizontally, and aluminum mechanical supports (Fig. 8c & d) were fixed to the biconical buoys' internal surface. The PV panels were placed and fixed to the upper surface of the biconical buoys (Fig. 8b), and holes were drilled to insert the PV cables. Then, cables were connected (Fig. 8d), and two strings (5 modules connected in series) were wired and subsequently connected to the MPPT (Fig. 9), to optimize the energy harvesting and accumulation process.

The storage management section is fundamental, and it is intended to accumulate the energy captured by the energy harvester and, at the same time, must be able to sustain adequate power to all the active electronic components present in the device. While a LiPo battery was used in the project. The battery has been connected to the energy harvesting system, which will manage to optimize the battery function. The battery and energy harvesting circuit board are housed inside the white case (Fig. 8c) which is of IP67.

The air temperature sensor, water temperature sensor, water pH sensor, and water salinity sensors were positioned at the bottom part (Fig. 8g) of the buoy within some protective tubes fixed to the buoy using marine silicon and two-component resin. The electrical cables were connected to the Water quality measurement and communication electronic device, which was placed inside a dark colored box (Fig. 8f).

Subsequently, two boxes with various electronic components were rigidly tied to each other and were mounted on aforesaid metallic supports (Fig. 8e). Finally, a circular metal structure was made to fix the two halves of the buoy, anchored with stainless steel screws to the edges of the structure. In order to make the buoys waterproof, several layers of marine silicon were applied to the central circumference of the buoy.

Once the marine silicon dried, several buoy tightness tests were performed, and subsequently functionality tests were conducted (Fig. 8h). During the tests, the operation of the electronics was monitored using the LoRaWAN communication system, sending the data

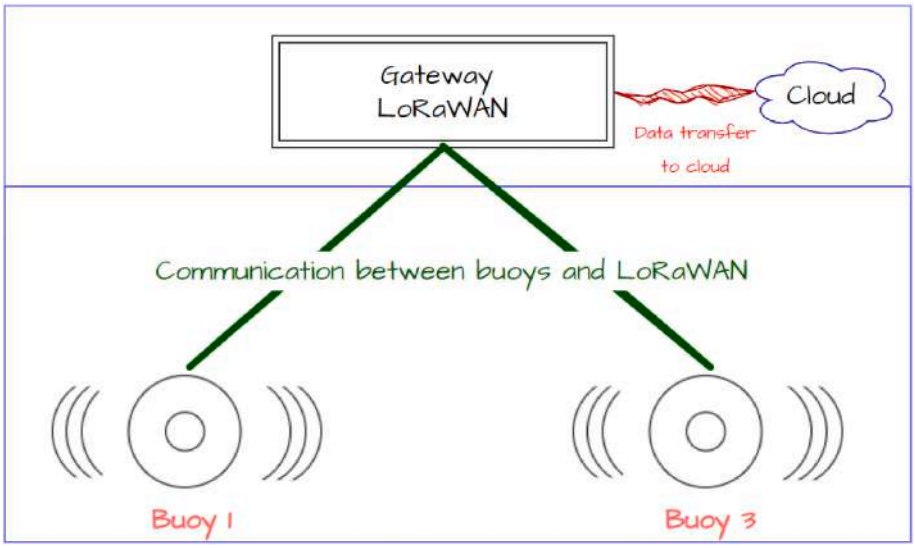

Fig. 6. General scheme of the communication system.

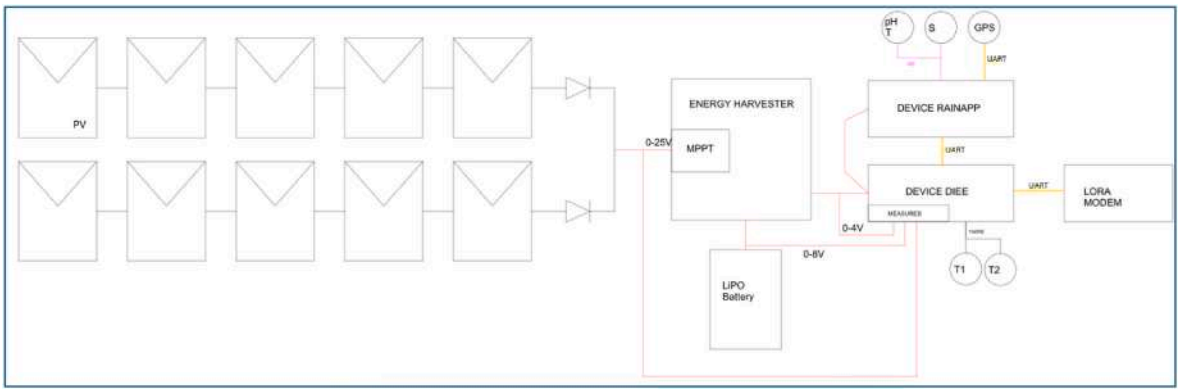

Fig. 7. Schematic diagram of the buoy.

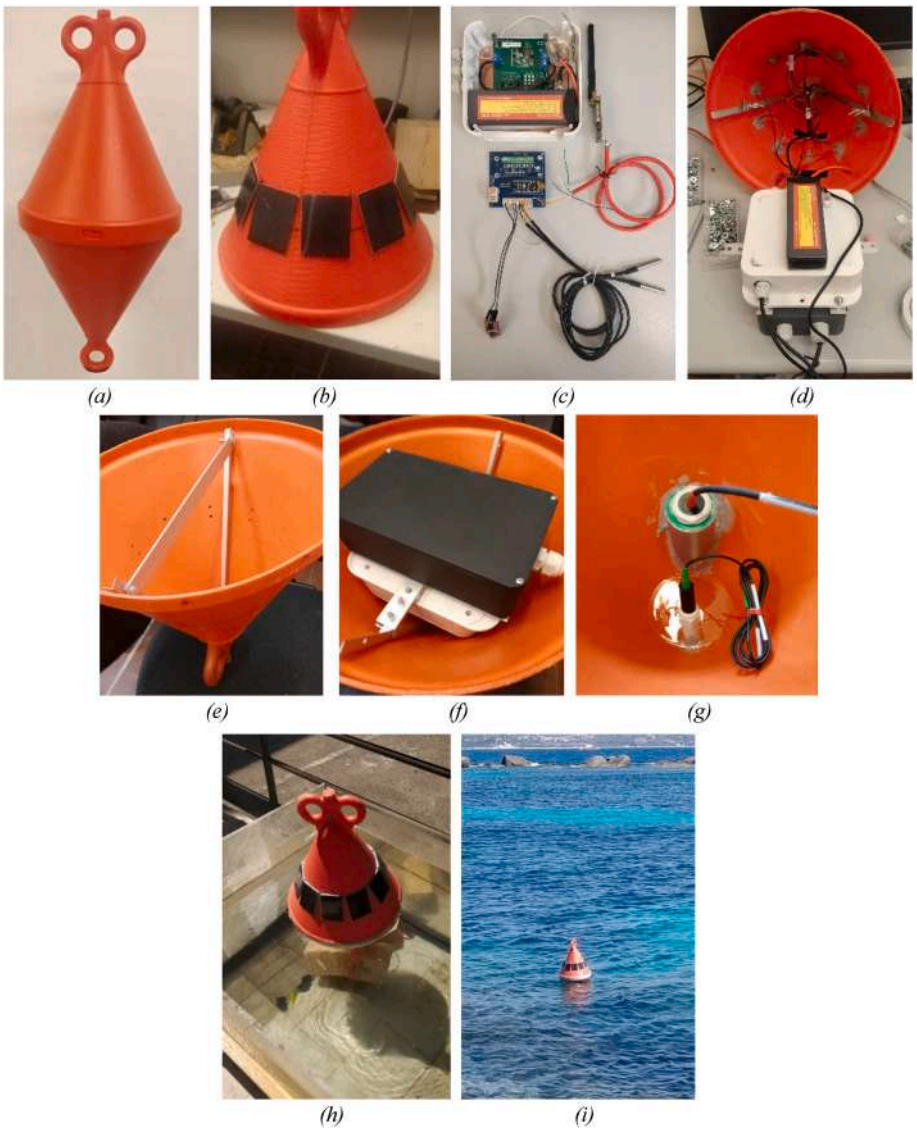

Fig. 8. (a) Buoy floating structure, (b) PV installation, (c)&(d) various sensors, electronic devices, and battery, (e) metal installation structure, (f) installation of electronic devices cases, (g) sensor installation, (h) Initial Lab test and (f) Prototype installation.

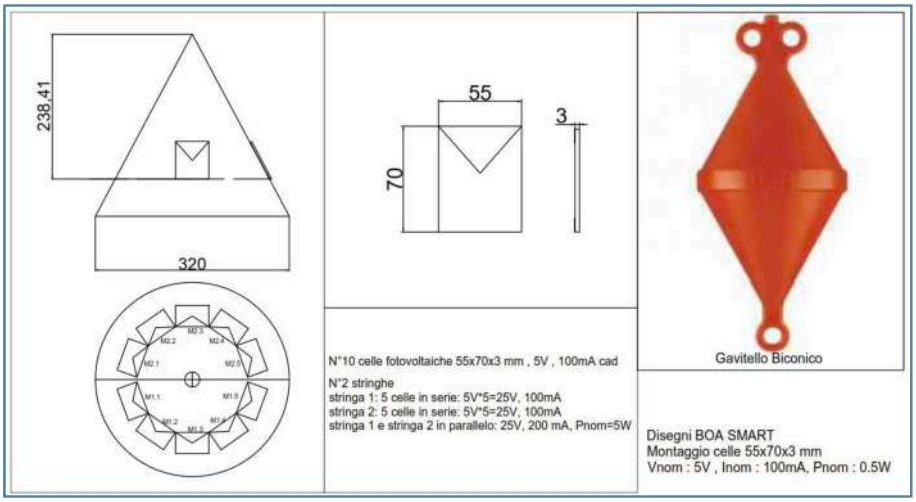

Fig. 9. PV modules installation scheme on the buoy.

packets to the LoRa gateway located inside the DIEE laboratory at the UniCA, Italy. In order to allow easy reading, the company IT Euromedia has made available an interface for monitoring the electrical parameters and the two internal temperatures of the buoy. An additional graphic interface has also been created for the monitoring of the environmental parameters and geolocation of the device.

2.2. PV panel, installation scheme and characterization

The PV system has been chosen for energy harvesting for its reliability and easy installation. Notably, it has already been proved that the PV modules can harness more energy when they are installed near, on, or above the water surface (Majumder et al., 2021) (Majumder et al., 2023). The buoys have been fitted with 10 PV modules with a nominal power of 0.5W, whereas the voltage and current at Maximum Power Point (MPP) are equal to 5V and 100 mA, respectively. As specified by the manufacturer, the dimensions of PV modules are "70 mm × 55 mm × 3 mm". The modules were placed at equidistance on the buoy in a circular pattern, and their installation scheme on the buoy is shown in Fig. 9. As presented in Fig. 7, two strings, each containing 5 modules, were connected in parallel (Fig. 7) to the input point of the energy harvesting system to maximize energy production. PV cables were inserted through holes, and the holes were sealed with marine silicon (a waterproofing and fastening element). The cables were welded, and the joints were protected with appropriate insulation. The terminal poles of the two series were then connected to the harvesting board, where the BQ24650 chip was mounted.

PV module characterization was carried out under solar irradiation 1000W/m^2, 800W/m^2, 600W/m^2, 400W/m^2, and 200W/m^2 with the help of a solarimeter and a reference PV cell (Fig. 10), later based on the measured data, I-V curves are plotted (Fig. 11).

2.3. Energy harvesting circuit

In order to design the energy harvesting and storage system, the energy consumption associated with each installed device and their operating modes were determined. Notably, two modes were defined, i.e., normal and sleep modes, respectively, for normal operation of the devices and low power operation. The individual devices' response times were also identified to estimate the energy consumption of the whole system. Table 2 shows the measured and estimated data.

The chip Texas Instruments' BQ24650 has been selected for energy harvesting to track the MMP of the PV system and to manage the battery's pre-charge and charging mode. It also helps to supply an output voltage to the load, depending on the battery charging state and the

Fig. 10. Workability verification of the Buoy system.

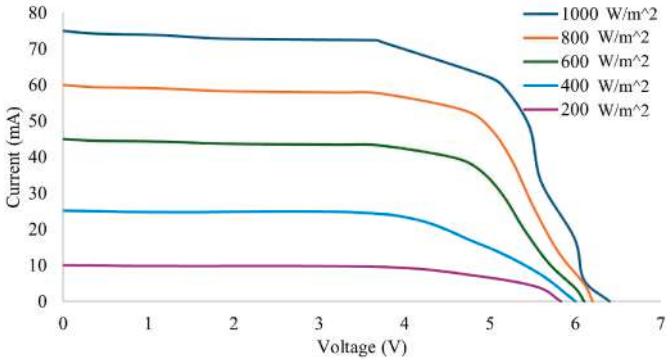

Fig. 11. I-V curves.

generation capability from the renewable source. The selected chip has a constant-frequency synchronous PWM controller with high-precision current and voltage regulation, charge preconditioning, charge termination, and charge status monitoring. The harvester supports a 2.1V–26V battery with voltage feedback set to a reference of 2.1V. The charging current is programmed by selecting an appropriate sensing resistor. The BQ24650 comes with a slim 16-pin, 3.5 mm × 3.5 mm Quad Flat No-lead (QFN) package. The device charges the battery in three stages: preconditioning, constant current, and constant voltage. The pre-charge timer is set at 30 min. The BQ24650 automatically restarts the charge cycle if the battery voltage drops below an internal threshold and enters low quiescent current sleep mode when the input voltage drops below the battery voltage. The typical diagram of the connection and configuration of the device is shown in Fig. 12.

The energy harvesting circuit parameters are, $R_{sr} = 200$ mΩ, corresponding $I_{charge} = 200$ mA and $I_{pre\text{-}charge} = 20$ mA. $R_3 = R_{17} = 499$ kΩ, $R_4 = R_{19} = 32.73$ kΩ (36 kΩ ‖ 360 kΩ), corresponding $V_{MPPset} = 19.49$V. $R_2 = R_{13} = 255$ kΩ, $R_1 = R_{15} = 90.90$ kΩ (100 kΩ ‖ 1MΩ resistor), corresponding $V_{bat} = 7.99$V. The reason for choosing these parameters is because the single PV module has a nominal voltage of about 5V, and the string is composed of 5 modules connected in series, thus obtaining a string voltage of about 25V in the condition of maximum irradiation. Let's consider a working voltage of 75% to get 18.75V and a second value of 80% to get 20V. Therefore, by choosing the values of R_{17} and R_{19} as described above (commercial values) we obtain a V_{MPPset} voltage equal to 19.49V which falls within the range between 75% and 80% of the maximum string voltage. The identified battery has a nominal voltage of 7.40V, so we set a slightly higher V_{bat} by setting the values of R_{13} and R_{14} to have $V_{bat} = 7.99$V.

2.4. Bi-directional current/power monitoring chip

A bidirectional current/power monitoring chip has been used to gather data related to the electricity consumption of various devices installed in the buoys and to perform a comparison. This chip has been instrumental in measuring the electrical operational parameters of the entire device, allowing for a timely assessment of the different devices installed in the buoys, even when they may be working in different conditions.

2.5. DIEE device diagram

Fig. 13 depicts the electrical board design used in weather buoys for data acquisition, measurements, and transmission. The Arduino microcontroller will be responsible for reading data from various sensors and storing them internally using different protocols. It will use the 1-wire protocol to read data from two temperature sensors, the I2C protocol to read data from the 4-channel electrical quantity measurement board (voltage and current from PV, system voltage and current, voltage and current from the battery, voltage and current of the water quality

Table 2
Consumption calculations.

Sensor	Sensor Readout Activity Time	Current	Adj. current	Voltage	Response time	Sleep	Sleep Time	Consumption per day reading	Consumption per day sleep
	s	mA	mA	V	s	mA	s	**Wh**	**Wh**
PH	4	35	22	3,3	1	0,995	86304	0,0050	0,0787
Temperature	4	35	22	3,3	1	0,09	86304	0,0050	0,0071
Salinity	4	57	22	3,3	1	0,4	86304	0,0070	0,0316
GPS	120	67	x	3,3	n.a.	0	83520	0,1769	0,0000
LoRa	180	128	x	3,3	2	0,104	82080	0,5069	0,0078
Total	x	322	388	3,3	x	1589	x	0,7007	0,1253
Total yearly								255,77156	45,7367922

WORKING HYPOTHESIS
- Each sensor is active for 4 s, then sleep mode
- GPS activates for 120 s for location acquisition and then is turned off/sleep
- The Arduino LoRa microcontroller comes out of sleep and remains active for 180 s (to acquire GPS position and sensor data)

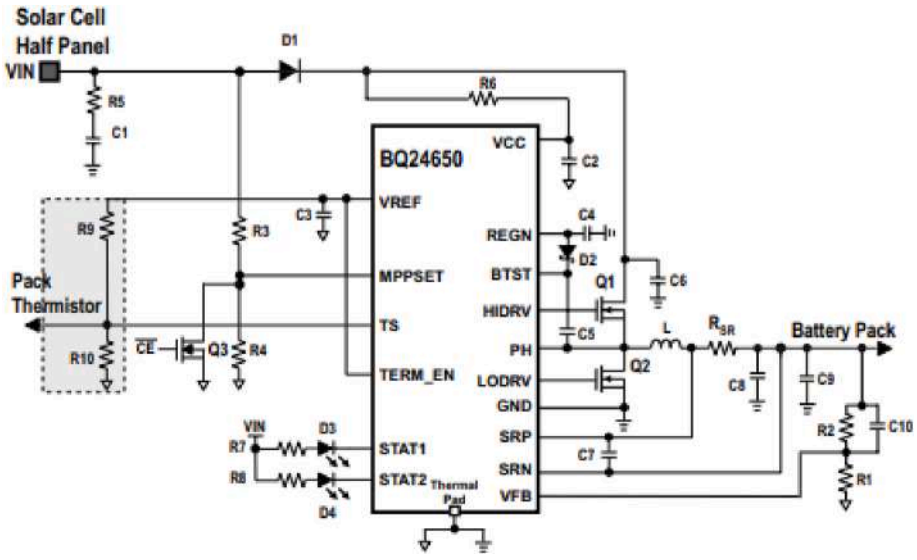

Fig. 12. Energy harvesting circuit.

measurement and communication device), and Serial communication (UART) to read from the water quality measurement and communication device, as well as send activation and deactivation commands (sleep mode ON/OFF) to the water quality measurement and communication device. Additionally, the stored data from all the sensor modules will be communicated through the LoRa network via the serial port.

Fig. 14 represents the Printed Circuit Board (PCB) relating to the electronic card described above. In Fig. 14 the area of the Current Monitor Strip (CMS) can be seen. It is made up of a board with four INA219 chips for measuring electrical quantities. The chips communicate with the I2C protocol, in which each chip is configured with its own I2C address. The four chips communicate with the Arduino microcontroller through the two SDA and SCL lines in fast mode (400kbps).

2.6. Microcontroller

In the project, it was decided to separate the power management and communication system by using the LoRaWAN protocol: (1) the part of environmental data acquisition and (2) GPS position detection, respectively. Therefore, multiple controllers have been used for different functionalities, such as the controller dedicated to the monitoring of consumption, the measurement of the temperature inside the buoy (air), the management of LoRaWAN communication, and the management of the acquisition board of environmental parameters consisting of an ATMega328P microcontroller installed on an Arduino board. Fig. 15 shows the central device connected to all the other devices inside the smart buoy.

The microcontroller communicates with the sensor and communication modules in the following ways: I2C communication is used to communicate with four INA219 modules, with the microcontroller acting as the master and the modules as slaves. The microcontroller collects temperature values from two temperature areas using the 1wire protocol. Serial communication (UART) is employed to collect water quality measurements and communicate with a device dedicated to acquiring environmental parameters such as pH, temperature, salinity of seawater, and GPS position. Additionally, serial communication is used to send the collected data through LoRaWAN. The serial port can also be used for testing, debugging, and updating the code.

2.7. Internal communication system

Notably, there are three different types of communication systems within the electronic device.

(1) Serial (UART): This is used for communication between the DIEE device and the LoRA modem and between the DIEE device and the water quality measurement and communication device. Within the water quality measurement and communication device, the same communication protocol is used for GPS communication.
(2) I2C: It is used inside the DIEE device to communicate with the INA219 devices and acquire electrical quantity readings. The

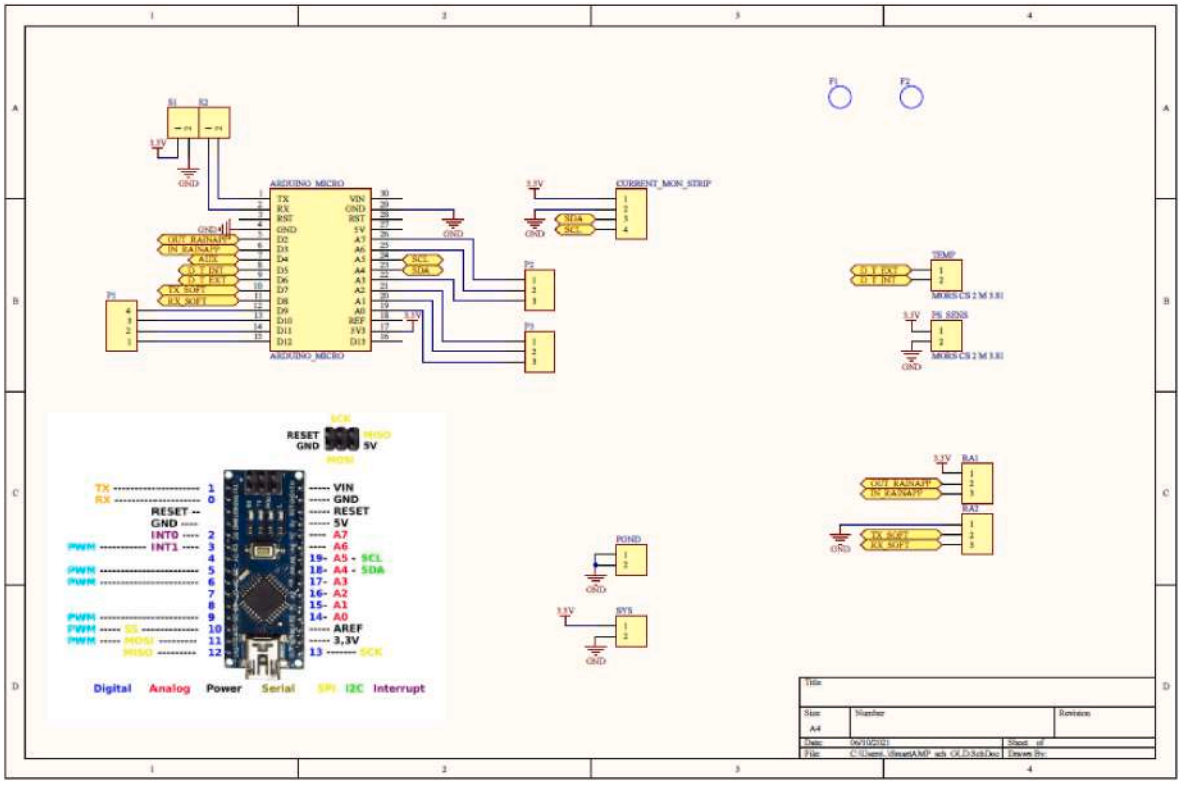

Fig. 13. Electric schemes of the components.

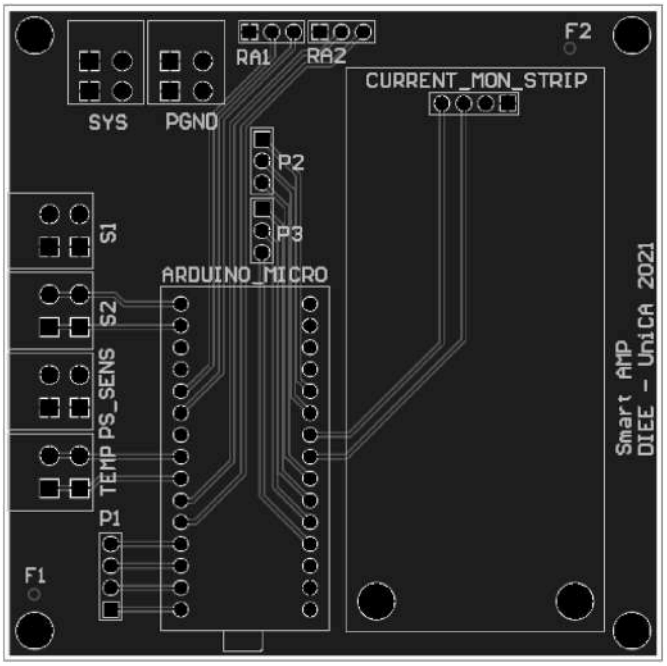

Fig. 14. PCB (Printed circuit board.

same protocol is also used within the Water quality measurement and communication device to acquire values from pH/temperature and salinity sensors.

(3) 1WIRE: It is used exclusively inside the DIEE device to communicate with the two temperature sensors inside the buoy.

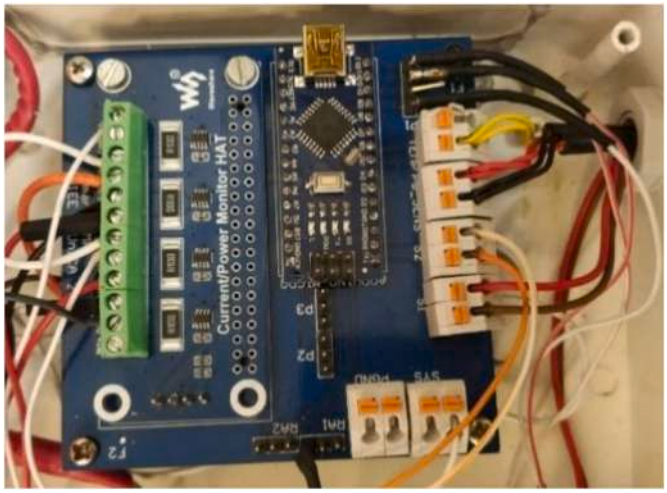

Fig. 15. Microcontroller.

2.8. Bouy to gateway communication system: LoRa and LoRaWAN

A highly innovative and emerging technology for long-range communications was used during the project, i.e., LoRa technology. LoRa uses a spread spectrum modulation technique that derives from CSS technology. The following image shows a sequence of transmitted (up-chirp) and encoded (down-chirp) data (see Fig. 16).

Small-sized, long-range, low-power single-chipset LoRa devices have been selected for this project. The system was equipped with a LoRa device in end device mode, which allows remote communication with the gateway located along the coast. The LoRa device is mounted on a miniaturized chip and performs the functions of a modem. Provisions are made that the data will be transmitted from the microcontroller to

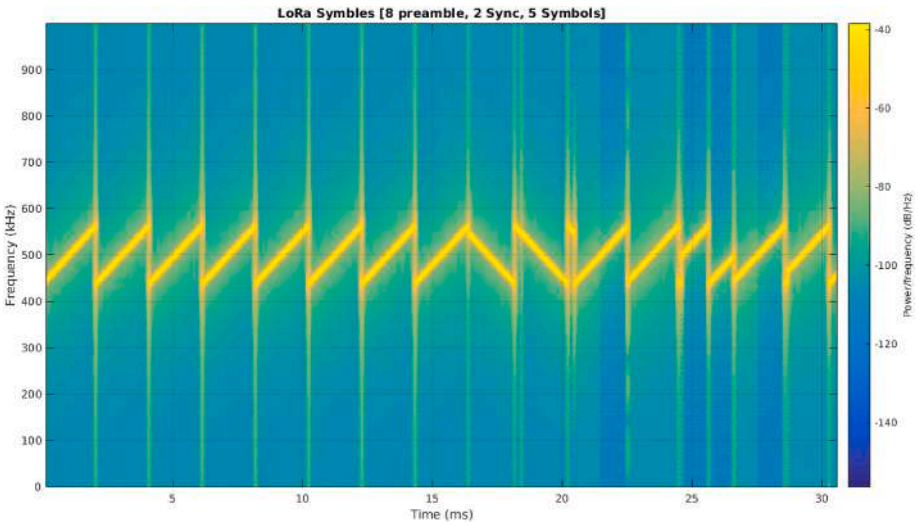

Fig. 16. Bouy to Gateway communication.

the LoRa modem via the UART port.

2.9. Cloud storage

The instantaneous data collection and temporary data storage are taken care of by the microcontroller on the buoy. The ultimate aim is to have a collective database for an enhanced understanding of the parameters monitored. A secondary and large storage system is required for the purpose and advancement in IoT and cloud storage aids in this aspect. In addition to storing the collected data, these cloud platforms come with different supporting elements like IoT connectivity, device management, application enablement, and analytics, which enhance and enrich the data management process (P et al., 2023), (Santhosh et al., 2021). These platforms also manage communication protocols to connect with devices using the internet, Wi-Fi, and Bluetooth, ensuring reliable data transfer. There are numerous such service providers from which "ThingsBoard" platform has been utilized; it is preferred as it is an open-source platform and offers sustainable scaling options.

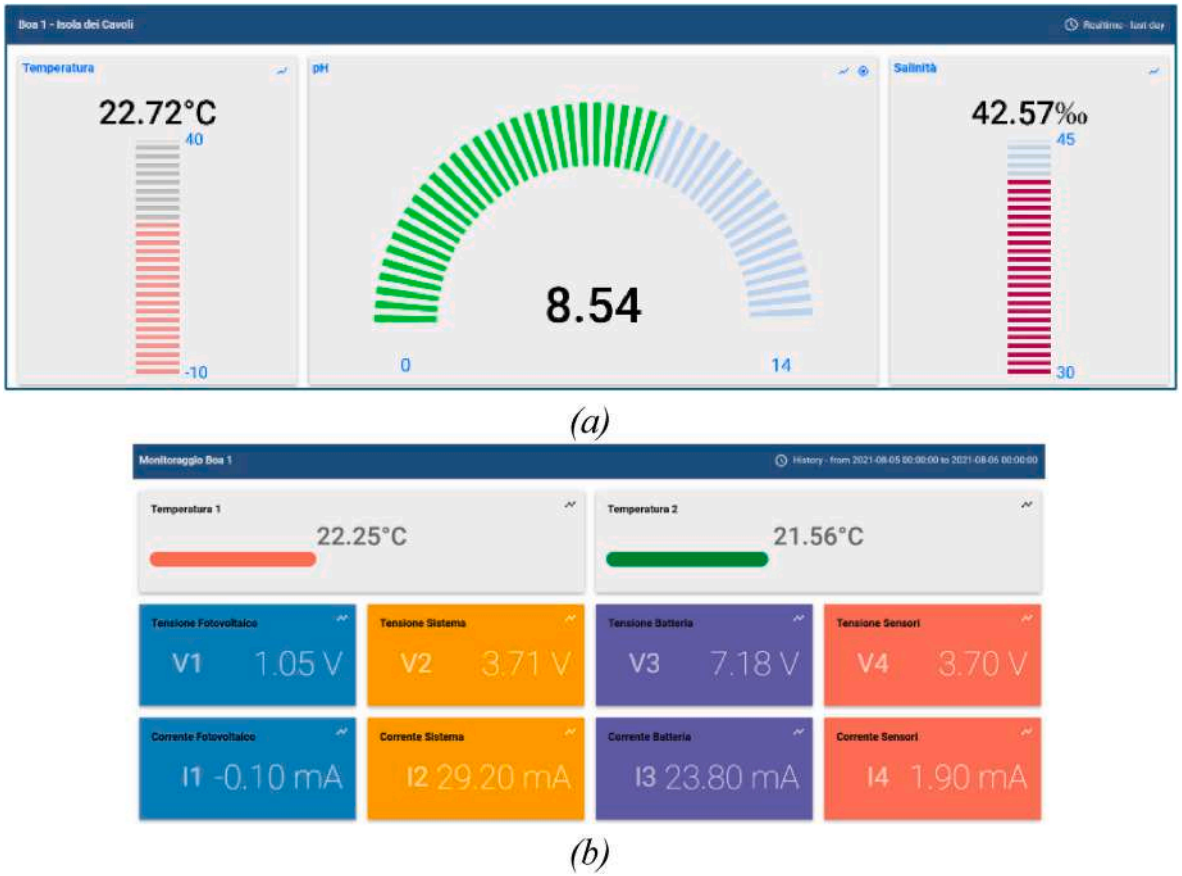

Fig. 17. Buoy 1. (a) Sensor measuring parameters, and (b) System measuring parameters.

2.10. Graphic User Interface (GUI)

During the development phase, it was decided to measure and send electrical parameters every 10 min. The measured environmental data and GPS position will be sent every hour. Notably, the RainAPP device will be put in sleep mode during periods of inactivity. Figs. 17 and 18 represents real-time measurements by the sensors and devices installed in buoy 1 and buoy 3.

3. Results

The refined data for a 7-day time frame of summer days has been presented in the following. Figs. 19 and 20 represent the relation between the PV system's corresponding voltage and current produced by the PV system, respectively, during the daytime within the selected time frame. Whereas Figs. 21 and 22 present the operation of the powered system. While from Figs. 24 and 25, it is possible to understand the charging and discharging cycles of the battery.

Notably in Fig. 19 it is clearly visible that the MPP Tracker (MPPT) algorithm activates and deactivates the energy harvester, maintaining a voltage of around 7V. Fig. 20 presents the hourly trend of the current supplied by the PV field.

Once this activation voltage is exceeded, the MPPT regulates the voltage and current at the MPP, which are 24.11V and 50 mA, respectively. Interestingly, on 16th August, due to bad weather, the PV system worked fewer hours. The minimum and average measured voltages are 1.01V and 10.93V, respectively. The average produced current during this period is about 15.17 mA.

Figs. 21 and 22 represent the voltage and current values measured for the system's total load. As in Figs. 21 and 22 the system voltage and current oscillate depending on the operating state of the PV field, this is due to the change in the functioning of the charging cycle and the discharging cycle of the battery. The maximum, minimum, and average current consumed by the system during this period is 31.1 mA, 27.2 mA, and 28.2 mA. Meanwhile, the same system's maximum, minimum, and average measured voltages for the same period are 4.07V, 4.03V, and 4.04V, respectively.

Although the buoy was designed to harvest with a maximum capacity of $5W_{peak}$, the buoy system has never reached the designed value, even on a sunny day with maximum solar irradiance. This was because PV panels were placed in a circular pattern, and all 10 panels were never exposed to the sun together (as shown in Fig. 23).

It is clear from the graph (Fig. 24) that during daylight hours, the battery voltage increases as the harvesting device generates more power than that absorbed by the load, and the excess is used to charge the storage system. Whereas from Fig. 25 it can be deduced that the current becomes negative (current entering the battery), causing the battery to be charged throughout the day.

During the night period, with the PV field disabled, the system uses only the energy accumulated in the battery, which delivers a current measured with a positive sign (current coming out of the battery). For the aforesaid observation period, the maximum, minimum, and average current of the battery, measured to be 73.3 mA, 24.6 mA, and 4.46 mA, respectively. Whereas the maximum, minimum, and average voltage were found to be 7.22V, 7.44V, and 7.32V, respectively.

Internal temperatures of the buoy, the upper part and the lower part are presented in Fig. 26 and 27 respectively. These data are acquired by the microcontroller and sent to the ThingsBoard cloud platform. The two sensors are placed inside the buoy, while the second sensor (Fig. 26) was put on the lower part of the buoy, which always remained submerged in the water. During this seven-day timeframe and for the month of May, the average daytime temperature obtained at the upper part of the buoy was about 41.84 °C, whereas for the lower part inside the buoy, it measured about 23.93°C.

Figs. 26–28, Figs. 29 and 30 represent measurements performed by the temperature, pH, and salinity sensors, respectively. The data presented in these graphs are taken from the timeframe between May 18, 2023 to May 24, 2023.

During the aforementioned time frame, the average seawater temperature was 23.8 °C (Fig. 28), pH was 8.61 (Fig. 29) and salinity was 36.62% (Fig. 30).

4. Future development

Based on the experience gained from aforesaid prototype buoy fabrication, the UniCA team is currently working on and developing a

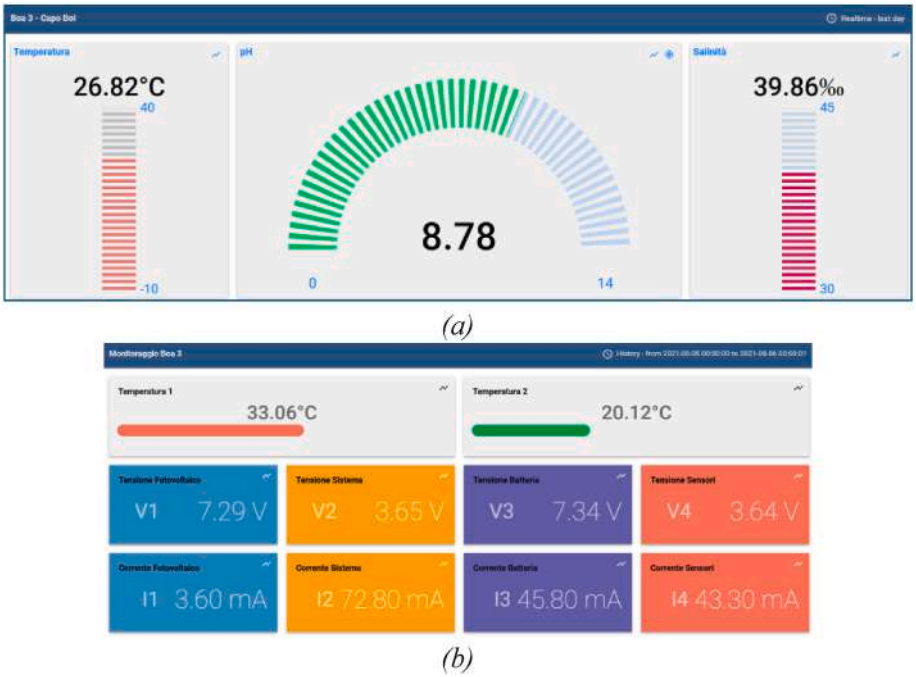

Fig. 18. Buoy 3 (a) Sensor measuring parameters, and (b) System measuring parameters.

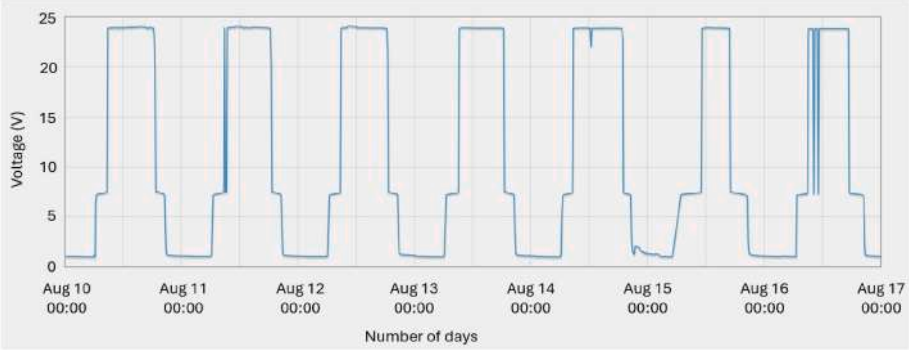

Fig. 19. Measured voltage at MPP.

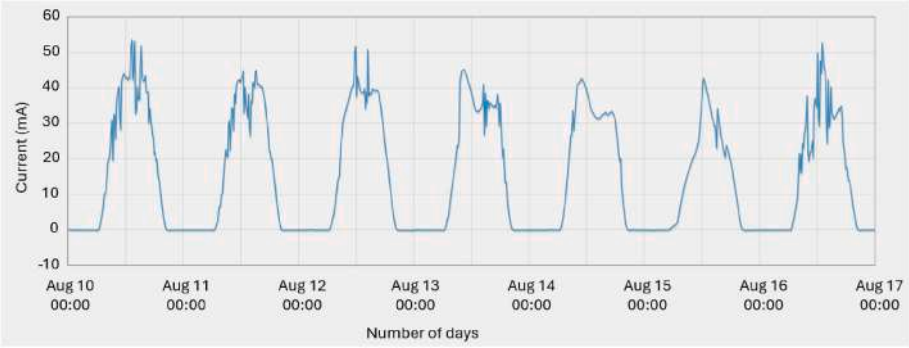

Fig. 20. Measured current at MPP.

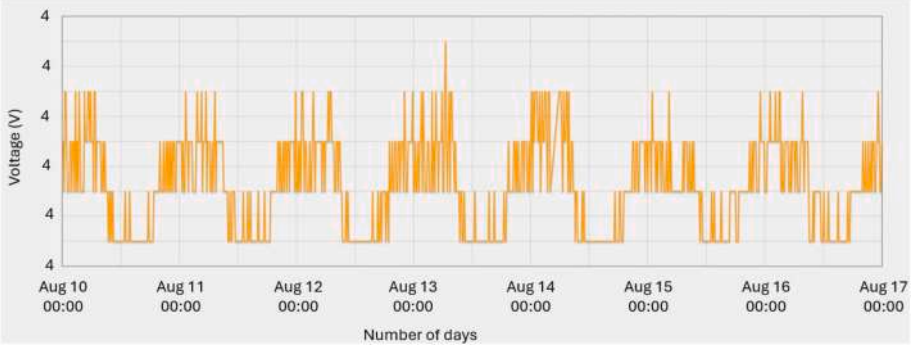

Fig. 21. Measured voltage of the system.

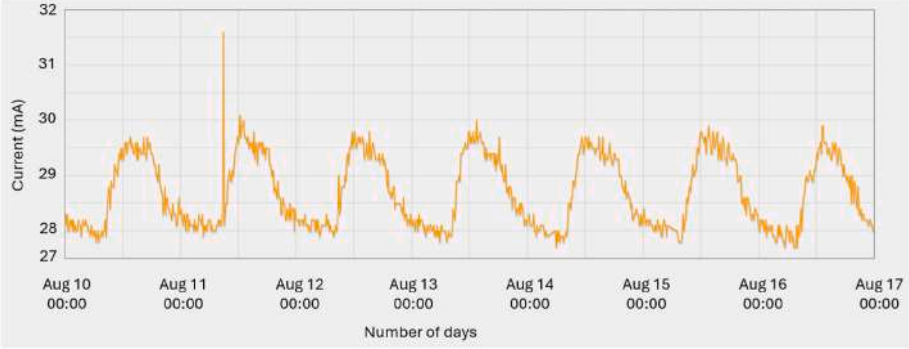

Fig. 22. Measured current of the system.

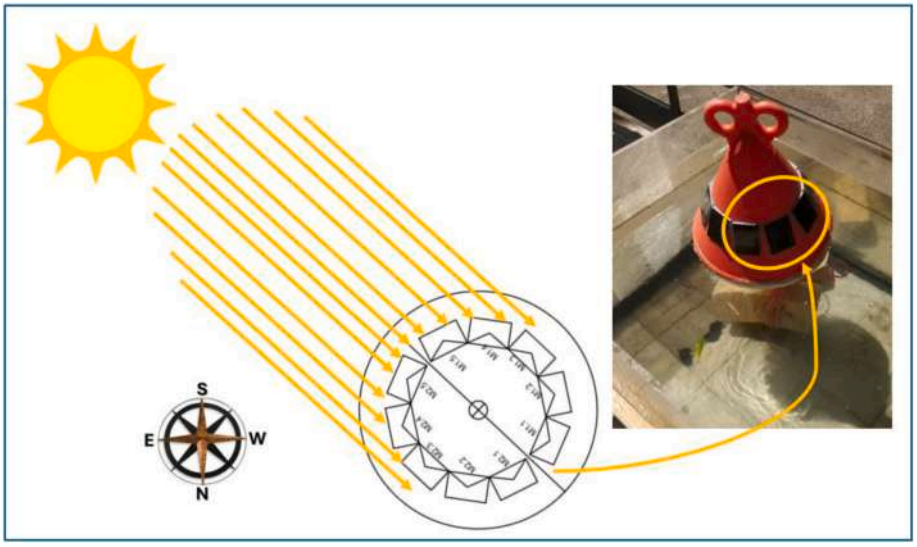

Fig. 23. Illustration of Energy harvesting of PV panels mounted on buoy.

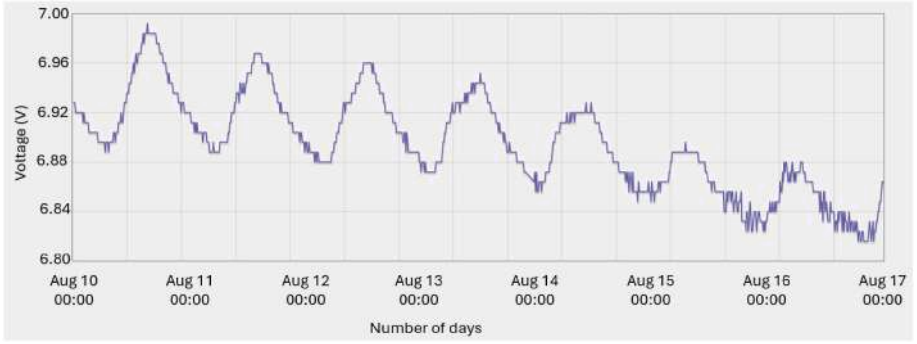

Fig. 24. Measured battery voltage.

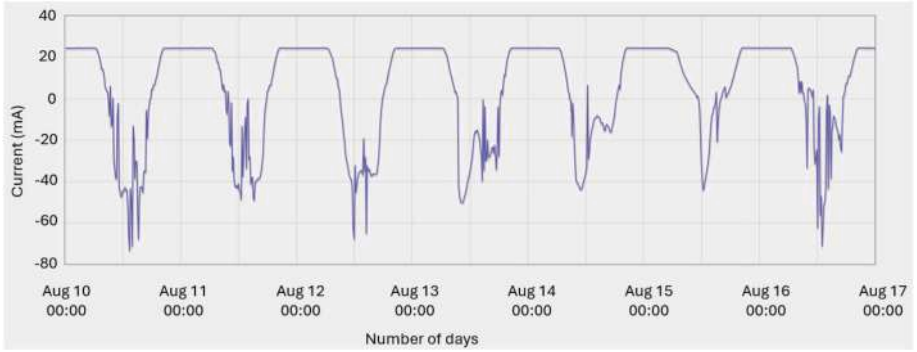

Fig. 25. Measured battery current.

smart weather station consisting of moored buoy (mother) and a portable buoy (daughter), as shown in Figs. 31 and 32.

The complete marine weather station package has two parts.

(1) Moored buoy: named as "MOTHER", is the fixed central operational and communication weather, and docking station to host the daughter buoy. The mother buoy is powered by a system composed of an energy generator from a PV source (and/or small wind turbine) and a maximum power point tracker (MPPT) would be used to optimize the direct current energy production. The produced energy would be stored in a $LiFePO_4$ battery system along with a super capacitor module (similar to the proposed model as in (Teasdale et al., 2024)). While an induction energy transmission system would be connected to the battery for charging the daughter buoy, the energy levels and other parameters of the battery in both mother and adaughter buoy are monitored through a battery management system (Santhosh et al., 2022) to ensure battery health. The battery would power all the electrical/electronic devices inside the mother buoy, and would regulate the power supply voltage via DC/DC converter to adapt the desired voltage level.

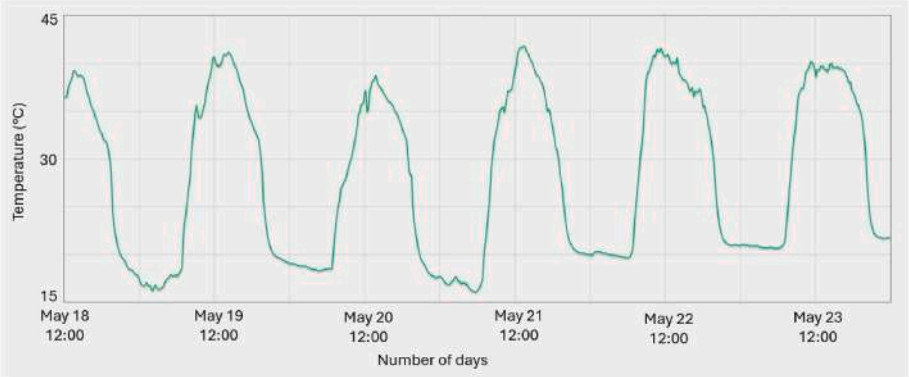

Fig. 26. Upper part temperature inside buoy.

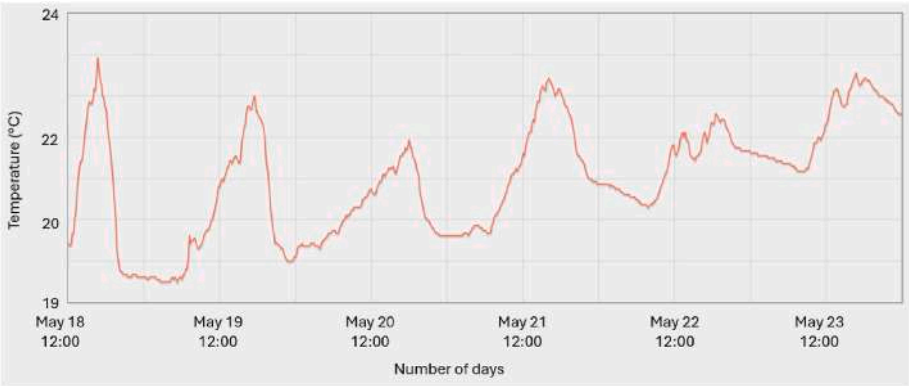

Fig. 27. Lower part temperature inside buoy.

Fig. 28. Water temperature.

The devices that are powered using the DC/DC converter are.

a) Microcontroller/microprocessor: It is the heart of the system and allows you to query all electronic devices via different communication protocols like I2C and UART. It also allows to send and receive digital signals from sensors and to communication devices.
b) sensors which works at a voltage of 3.3V and communicate with I2C or UART protocol
c) the LoRa device communicates with the microcontroller/microprocessor via UART protocol
d) the weather station communicates with UART protocol

(2) Autonomous surface crafts (ASCs): named as "DAUGHTER" is a moving weather station and capable of conducting various missions, it is an unmanned surface vehicle (USVs). The daughter buoy would be equipped with turbines to conduct long-distance missions, particularly to collect water samples to analyze the presence of micro-plastic with the aim of cleaning the water.

The daughter buoy is powered by a $LiFePO_4$ battery system, and it would be charged by an induction energy reception system from the mother buoy when it is connected (comes near to it). The battery would power all the electrical/electronic devices inside the daughter buoy and would regulate the power supply voltage via a DC/DC converter to adapt the desired voltage level. The devices that are powered using the DC/DC converter are.

a) Microcontroller/microprocessor
b) sensors which works at a voltage of 3.3V and communicate with I2C or UART protocol

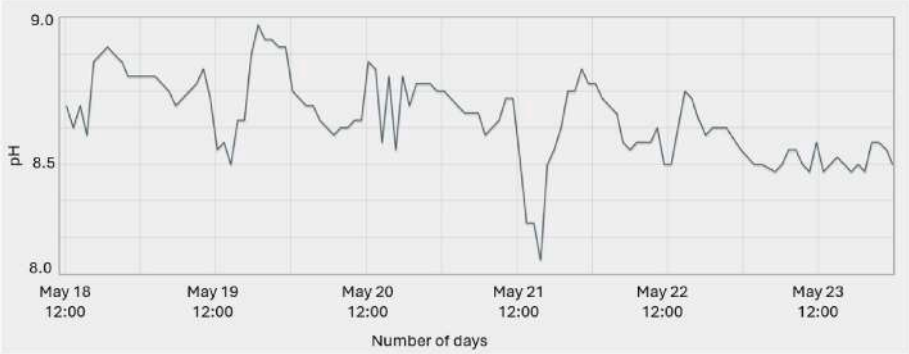

Fig. 29. pH of the sea water.

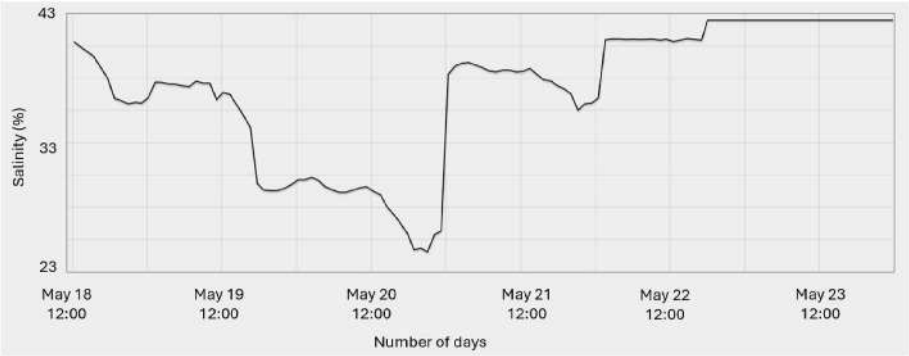

Fig. 30. The salinity of the seawater.

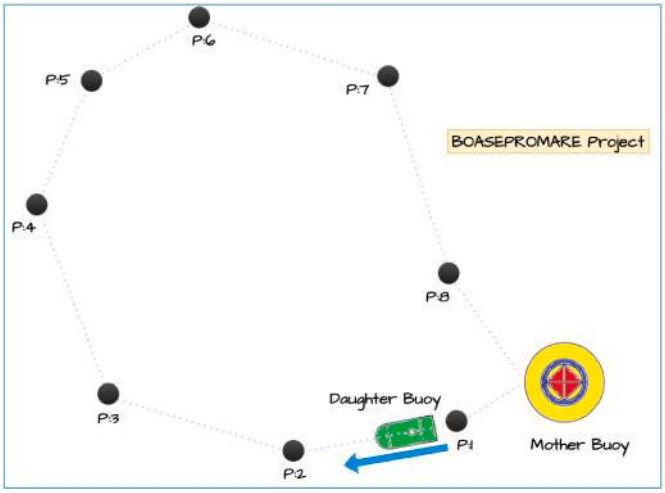

Fig. 31. Fixed Mother Buoy and movable Daughter Buoy.

c) the LoRa device communicates with the microcontroller/microprocessor via UART protocol
d) the weather station communicates with UART protocolthe GPS sends data to the microcontroller/microprocessor (in the mother buoy) in order to know the position of the device and calculate its route via the IMU
e) the autonomous driving system (software resident in the microcontroller/microprocessor) allows the trajectory of the mission to be calculated and the course corrected by activating the electric motors mounted inside the vessel, also based on the detection of obstacles (e.g. via Light detection and ranging (LIDAR) and underwater IP cam system)
f) the microplastic collection system can be electromechanical or simply mechanical, operated by an appropriate electronic control system
g) the GPS/GNSS system is also used in case of emergency in order to know the position (or last known position) of the vessel in order to plan any recovery missions

5. Conclusion

This research focused on designing lightweight, energy-efficient, and self-sustaining weather buoys. These buoys have sensors and tracking instruments to collect meteorological data and location information, and a wireless communication device is used to transmit data through a LoRaWAN gateway, which allows for efficient data transmission and power conservation. The buoys are designed to operate in areas with limited GSM coverage. Our research also aimed to study the feasibility of installing these buoys in shallow seawater and monitoring their performance in marine environmental conditions. For the first time, such buoys have been deployed in the marine protected area of Capo Carbonara, Sardinia, Italy, for environmental monitoring.

This research has areas that could be improved. The buoys were designed to generate up to $5W_{peak}$ but consistently fell short, possibly due to the circular arrangement of PV panels. Due to structural limitations, no wave measurement sensor or deepwater temperature profiling was possible. We acknowledge the current limitations and are committed to improving our research. We plan to enhance the buoys for our next project by adding extra sensors to boost their performance. The UniCA team is currently working on an advanced smart weather and docking station. This system comprises a stationary (mother) buoy, which will function as a continuous operational and communication hub for the portable (daughter) buoy. The daughter buoy will be responsible for conducting long-distance missions to collect water samples, assess microplastic levels, and act as a mobile weather station. These buoys

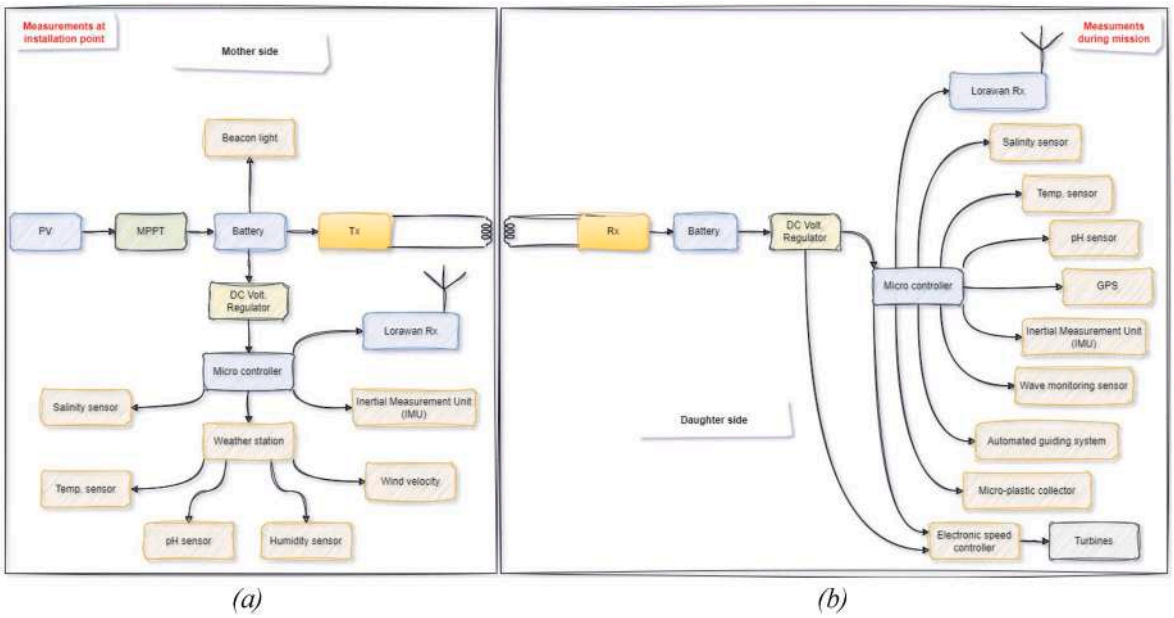

Fig. 32. Schematic diagram of installed instruments: (a) Mother side, and (b) Daughter side.

will be used to monitor the water around Sardinian Island and contribute to restoring the water ecosystem.

The research and development of prototype smart weather buoys, as well as the potential future development of a pair of mother-daughter weather buoys, directly contribute to the UN's Sustainable Development Goals (SDGs), precisely Goal 14, which focuses on conserving and sustainably using oceans, seas, and marine resources. These buoys can monitor water bodies like oceans, seas, and rivers, enabling us to assess and restore the health of local and global ecosystems.

CRediT authorship contribution statement

Arnas Majumder: Writing – review & editing, Writing – original draft, Methodology, Investigation, Formal analysis, Data curation, Conceptualization. **Michele Losito:** Writing – review & editing, Validation, Software, Resources, Investigation, Data curation, Conceptualization. **Santhosh Paramasivam:** Writing – review & editing, Visualization, Formal analysis. **Amit Kumar:** Writing – review & editing, Validation, Investigation, Formal analysis, Conceptualization. **Gianluca Gatto:** Writing – review & editing, Supervision, Project administration, Funding acquisition, Conceptualization.

Data availability statement

All data generated or analyzed during this study is included in this article. No additional data are available.

Declaration of competing interest

The authors declare that they have no known competing financial interests or personal relationships that could have appeared to influence the work reported in this paper.

Acknowledgement

This work was carried out within project "BoSeProMare", financed under Sardinia Regional Development Program 2020–2024, Strategy 2 ICT Sector, and "3SM – Smart Sea Santa Marinella" Regional Operational Program of the European Regional Development Fund (FESR) for the Lazio region PR-FESR 2021–2027.

References

Albaladejo, C., Soto, F., Torres, R., Sánchez, P., López, J.A., 2012. A low-cost sensor buoy system for monitoring shallow marine environments. Sensors 12 (7), 9613–9634. https://doi.org/10.3390/s120709613.

Amaechi, C.V., Wang, F., Ye, J., 2022a. Numerical studies on CALM buoy motion responses and the effect of buoy geometry cum skirt dimensions with its hydrodynamic waves-current interactions. Ocean Eng. 244, 110378. https://doi.org/10.1016/j.oceaneng.2021.110378.

Amaechi, C.V., Wang, F., Ye, J., 2022b. Investigation on hydrodynamic characteristics, wave–current interaction and sensitivity analysis of submarine hoses attached to a CALM buoy. JMSE 10 (1), 120. https://doi.org/10.3390/jmse10010120.

Amaechi, C.V., Wang, F., Ye, J., 2022c. Understanding the fluid–structure interaction from wave diffraction forces on CALM buoys: numerical and analytical solutions. Ships Offshore Struct. 17 (11), 2545–2573. https://doi.org/10.1080/17445302.2021.2005361.

Balaji, R., Sannasiraj, S.A., Sundar, V., 2006. Tsunami wave interaction with data buoys. Mar. Geodesy 29 (4), 235–251. https://doi.org/10.1080/01490410601008903.

Balakrishnan Nair, T.M., et al., 2024. An integrated buoy-satellite based coastal water quality nowcasting system: India's pioneering efforts towards addressing UN ocean decade challenges. J. Environ. Manag. 354, 120477. https://doi.org/10.1016/j.jenvman.2024.120477.

Bojic, F., Karin, I., Juricevic, I., Cipcic, M., 2021. Design and application of an automated smart buoy in increasing navigation safety and environmental standards in ports. TransNav 15 (2), 373–380. https://doi.org/10.12716/1001.15.02.14.

Chen, S., et al., 2023. Structure design and implementation of a high stability semi-submersible optical buoy for marine environment observation. Ocean Eng. 290, 116217. https://doi.org/10.1016/j.oceaneng.2023.116217.

Chen, C., Huang, S., Tavakkolnia, I., Safari, M., Haas, H., 2024. Spatial and wavelength division joint multiplexing system design for MIMO-OFDM visible light communications. IEEE Access 12, 109526–109543. https://doi.org/10.1109/ACCESS.2024.3439407.

D, S.K., Sankar Panda, U., Pradhan, U., Mishra, P., Ramana Murthy, M.V., 2022. Assimilation of water quality buoy data for improved forecasting. In: OCEANS 2022 - Chennai. IEEE, Chennai, India, pp. 1–5. https://doi.org/10.1109/OCEANSChennai45887.2022.9775448.

Darlis, A.R., Cahyadi, W.A., Chung, Y.-H., 2018. Shore-to-Undersea visible light communication. Wireless Pers. Commun. 99 (2), 681–694. https://doi.org/10.1007/s11277-017-5136-9.

Elipot, S., Sykulski, A., Lumpkin, R., Centurioni, L., Pazos, M., 2022. A dataset of hourly sea surface temperature from drifting buoys. Sci. Data 9 (1), 567. https://doi.org/10.1038/s41597-022-01670-2.

Fathi, M., Haghi Kashani, M., Jameii, S.M., Mahdipour, E., 2022. Big data analytics in weather forecasting: a systematic review. Arch. Comput. Methods Eng. 29 (2), 1247–1275. https://doi.org/10.1007/s11831-021-09616-4.

García, E., Quiles, E., Correcher, A., Morant, F., 2018. Sensor buoy system for monitoring renewable marine energy resources. Sensors 18 (4), 945. https://doi.org/10.3390/s18040945.

Hurst, T., Christenson, B., Cole-Baker, J., 2012. Use of a weather buoy to derive improved heat and mass balance parameters for Ruapehu Crater Lake. J. Volcanol. Geoth. Res. 235–236, 23–28. https://doi.org/10.1016/j.jvolgeores.2012.05.004.

Ju, X., Amaechi, C.V., Dong, B., Meng, X., Li, J., 2023. Numerical analysis of fishtailing motion, buoy kissing and pullback force in a catenary anchor leg mooring (CALM)

moored tanker system. Ocean Eng. 278, 114236. https://doi.org/10.1016/j.oceaneng.2023.114236.
Jung, H., et al., 2024. Self-powered ocean buoy using a disk-type triboelectric nanogenerator with a mechanical frequency regulator. Nano Energy 121, 109216. https://doi.org/10.1016/j.nanoen.2023.109216.
Kahn, J.M., Barry, J.R., 1997. Wireless infrared communications. Proc. IEEE 85 (2), 265–298. https://doi.org/10.1109/5.554222.
Kim, S.M., Lee, U.H., Kwon, H.J., Kim, J.Y., Kim, J., 2017. Development of an IoT platform for ocean observation buoys. IEIE Transactions on Smart Processing and Computing 6 (2), 109–116. https://doi.org/10.5573/IEIESPC.2017.6.2.109.
Kington, J.A., Selinger, F., 2006. The development and use of weather buoys 1940–2005. Weather 61 (6), 164–166. https://doi.org/10.1256/wea.247.05.
Klemas, V., 2011. Remote sensing of Sea Surface salinity: an overview with case studies. J. Coast Res. 276, 830–838. https://doi.org/10.2112/JCOASTRES-D-11-00060.1.
Knight, P.J., Bird, C.O., Sinclair, A., Higham, J., Plater, A.J., 2021. Beach deployment of a low-cost GNSS buoy for determining sea-level and wave characteristics. Geosciences 11 (12), 494. https://doi.org/10.3390/geosciences11120494.
Kodaira, T., et al., 2024. An affordable and customizable wave buoy for the study of wave-ice interactions: design concept and results from field deployments. Coast Eng. J. 66 (1), 74–88. https://doi.org/10.1080/21664250.2023.2249243.
I. Kuznetsov, 'What are weather buoys and where they are applied'. Accessed: August. 3, 2024. [Online]. Available:https://windy.app/blog/weather-buoys.html.
Lin, M., Yang, C., 2020. Ocean observation technologies: a review. Chin. J. Mech. Eng. 33 (1), 32. https://doi.org/10.1186/s10033-020-00449-z.
Lindsy, R.. Climate change: global sea level. https://www.climate.gov/news-features/understanding-climate/climate-change-global-sea-level. (Accessed 20 March 2024).
Majumder, A., Innamorati, R., Frattolillo, A., Kumar, A., Gatto, G., 2021. Performance analysis of a floating photovoltaic system and estimation of the evaporation losses reduction. Energies 14 (24), 8336. https://doi.org/10.3390/en14248336.
Majumder, A., et al., 2023. Cooling methods for standard and floating PV panels. Energies 16 (24), 7939. https://doi.org/10.3390/en16247939.
Malek Azari, M., Salazar Luces, J.V., Hirata, Y., 2020. Design, assessment and evaluation of structural stabilization system for weather buoys using a moving foil. Robomech J 7 (1), 30. https://doi.org/10.1186/s40648-020-00178-x.
Maritime Engineering Technology, UniKL MIMET, Perak, Malaysia, 2019. Floating Buoy Technology for Research Purposes', IJITEE 8 (12), 5514–5520. https://doi.org/10.35940/ijitee.L3967.1081219.
Martínez-Osuna, J.F., et al., 2021. Coastal buoy data acquisition and telemetry system for monitoring oceanographic and meteorological variables in the Gulf of Mexico. Measurement 183, 109841. https://doi.org/10.1016/j.measurement.2021.109841.
McLeod, I., Ringwood, J.V., 2022. Powering data buoys using wave energy: a review of possibilities. J. Ocean Eng. Mar. Energy 8 (3), 417–432. https://doi.org/10.1007/s40722-022-00240-3.
Nilo, M.A., 2020. Long range communication technology for weather buoy. IJETER 8 (8), 4399–4404. https://doi.org/10.30534/ijeter/2020/58882020.
NOAA, P.M.E.L., McPhaden, M., Connell, K., Foltz, G., Perez, R., Grissom, K., 2023. Tropical Ocean observations for weather and climate: a decadal overview of the global tropical moored buoy array. Oceanog. https://doi.org/10.5670/oceanog.2023.211.
Oceanic Engineering Society and Marine Technology Society (Ed.), 2013. Oceans 2013: [conference] ; San Diego, California, USA, 23 - 27 September 2013. IEEE, Piscataway, NJ.
Olson, S., Jansen, M.F., Abbot, D.S., Halevy, I., Goldblatt, C., 2022. The effect of ocean salinity on climate and its implications for earth's habitability. Geophys. Res. Lett. 49 (10). https://doi.org/10.1029/2021GL095748.
Otero, P., Hernández-Romero, Á., Luque-Nieto, M.-Á., Ariza, A., 2023. Underwater positioning system based on drifting buoys and acoustic modems. JMSE 11 (4), 682. https://doi.org/10.3390/jmse11040682.
P, S., G, K., M, J., M, D., L, A.K., N, D., 2023. IoT based supervisory and diagnosis system for solar farm. 2023 9th International Conference on Advanced Computing and Communication Systems (ICACCS) 914–918. https://doi.org/10.1109/ICACCS57279.2023.10112993. Coimbatore, India.
Przybysz, A., Duarte, C.M., Geraldi, N.R., Kosel, J., Berumen, M.L., 2020. Cellular network marine sensor buoy. In: 2020 IEEE Sensors Applications Symposium (SAS). IEEE, Kuala Lumpur, Malaysia, pp. 1–6. https://doi.org/10.1109/SAS48726.2020.9220047.
Qin, H., Mu, L., Tang, W., Hu, Z., 2019. Numerical study of the interaction between peregrine breather based freak waves and twin-plate breakwater. J. Fluid Struct. 87, 206–227. https://doi.org/10.1016/j.jfluidstructs.2019.04.003.
Rabault, J., et al., 2022. OpenMetBuoy-v2021: an easy-to-build, affordable, customizable, open-source instrument for oceanographic measurements of drift and waves in sea ice and the open ocean. Geosciences 12 (3), 110. https://doi.org/10.3390/geosciences12030110.
Santhosh, P., Singh, A.K.S., Ajay, M., Gaayathry, K., Haran, H.S., Gowtham, S., 2021. IoT based monitoring and optimizing of energy utilization of domestic and industrial loads. In: 2021 5th International Conference on Intelligent Computing and Control Systems. ICICCS), Madurai, India, pp. 393–397. https://doi.org/10.1109/ICICCS51141.2021.9432121.
Santhosh, P., Arjunn, D., Daniel Dhas, A., Dinesh Kumar, M., Jeshwanth, S., Logesh, N., 2022. Remote monitoring and analysis of EV batteries using BMS. In: 2022 3rd International Conference on Smart Electronics and Communication (ICOSEC), Trichy, India, pp. 385–389. https://doi.org/10.1109/ICOSEC54921.2022.9952157.
Shukla, A., Matharu, P.S., Bhattacharya, B., 2023. Design and development of a continuous water quality monitoring buoy for health monitoring of river Ganga. Eng. Res. Express 5 (4), 045073. https://doi.org/10.1088/2631-8695/ad0d40.
Song, Y., Tong, Z., Cong, B., Yu, X., Kong, M., Lin, A., 2016. A combined Radio and underwater wireless optical communication system based on buoys. J. Phys.: Conf. Ser. 679, 012030. https://doi.org/10.1088/1742-6596/679/1/012030.
Soreide, N.N., Woody, C.E., Holt, S.M., 2001. Overview of ocean based buoys and drifters: present applications and future needs. In: MTS/IEEE Oceans 2001. An Ocean Odyssey. Conference Proceedings (IEEE Cat. No.01CH37295). Marine Technol. Soc, Honolulu, HI, USA, pp. 2470–2472. https://doi.org/10.1109/OCEANS.2001.968388.
Stohs, S.M., Harmon, K.M., 2022. Bayesian prediction of fishery biological impacts from limited data: a deep-set buoy gear case study. Fish. Res. 249, 106228. https://doi.org/10.1016/j.fishres.2022.106228.
Sun, Y., Wu, S., Chen, Y., Tu, Z., Yi, A., Yang, C., 2024. Disposable portable buoy for data transmission between seafloor equipment and onshore laboratories. Ocean Eng. 301, 117574. https://doi.org/10.1016/j.oceaneng.2024.117574.
Teasdale, A., Ishaku, L., Amaechi, C.V., Adelusi, I., Abdelazim, A., 2024. A study on an energy-regenerative braking model using supercapacitors and DC motors. World Electr. Veh. J. 15, 326. https://doi.org/10.3390/wevj15070326.
The proceedings of the twenty-first, 2011. International Offshore and Polar Engineering Conference: Maui, Hawaii, USA, June 19-24, 2011. International Society of Offshore and Polar Engineers, Cupertino, Calif, 2011.
Thomson, J., et al., 2024. Development and testing of microSWIFT expendable wave buoys. Coast Eng. J. 66 (1), 168–180. https://doi.org/10.1080/21664250.2023.2283325.
US Dept of Commerce, 'National Data Buoy Center Stations', National Data Buoy Center, National Oceanic and Atmospheric Administration, US Dept of Commerce. Accessed: March. 31, 2024. [Online]. Available: https://www.ndbc.noaa.gov/obs.shtml.
Verma, J., Pant, H., Sing, S., Tiwari, A., 2020. Marine pollution, sources, effect and management. Three Major Dimensions of Life: Environment, Agriculture and Health; Society of Biological Sciences and Rural Development: Prayagraj, India 270–276.
Winchester, J.W., 1974. Development of environmental data buoys. Nav. Eng. J. 86 (4), 97–109. https://doi.org/10.1111/j.1559-3584.1974.tb03680.x.
Xie, X., Wei, Z., Wang, B., Chen, Z., Oltmanns, M., Song, X., 2022. Extreme air–sea turbulent fluxes during tropical cyclone Barijat observed by a newly designed drifting buoy. Fundamental Research. https://doi.org/10.1016/j.fmre.2022.08.022. S2667325822003661.
Xu, G., Shen, W., Wang, X., 2014. Applications of wireless sensor networks in marine environment monitoring: a survey. Sensors 14 (9), 16932–16954. https://doi.org/10.3390/s140916932.
Xu, R., Wang, H., Xi, Z., Wang, W., Xu, M., 2022. Recent progress on wave energy marine buoys. JMSE 10 (5), 566. https://doi.org/10.3390/jmse10050566.
Zhong, Y.-Z., Chien, H., Chang, H.-M., Cheng, H.-Y., 2022. Ocean wind observation based on the mean square slope using a self-developed miniature wave buoy. Sensors 22 (19), 7210. https://doi.org/10.3390/s22197210.
Goal 14: Life below water: conserve and sustainably use the oceans, seas and marine resources for sustainable development. https://www.unep.org/explore-topics/sustainable-development-goals/why-do-sustainable-development-goals-matter/goal-14. (Accessed 20 March 2024).
World Ocean circulation experiment (WOCE), National Centers for Environmental Information. Accessed: March. 20, 2024. [Online]. Available: World Ocean Circulation Experiment (WOCE).